

Determination of optimal nanotube radius for single-strand deoxyribonucleic acid encapsulation

Mansoor H. Alshehri, Barry J. Cox, James M. Hill

Nanomechanics Group, School of Mathematical Sciences, University of Adelaide, Adelaide, SA 5005, Australia
E-mail: mansoor.alshehri@adelaide.edu.au

Published in Micro & Nano Letters; Received on 24th October 2013; Accepted on 20th December 2013

The molecular interactions between a single-strand deoxyribonucleic acid (ssDNA) molecule and a carbon nanotube (CNT) are modelled to determine the suction force experienced by the DNA which is assumed to be located on the axis near the open end of a single-walled CNT (SWCNT). They determine the optimal nanotube radius for encapsulation, that is, the radius of the nanotube with the lowest interaction energy. The expression for the molecular interaction energy is derived from the 6–12 Lennard-Jones potential together with the continuum approach, which assumes that a discrete atomic structure can be replaced by a line or a surface with constant average atomic density. It was found that an ssDNA can be encapsulated inside a SWCNT with a radius larger than 8.2 Å, and it is shown that the optimal SWCNT needed to fully enclose the DNA molecule has a radius of 8.8 Å, which approximately corresponds to the chiral vector numbers (13, 13). This means that if it is wished to encapsulate the ssDNA into a CNT, an ideal SWCNT to do this is (13, 13) which has the required radius of 8.8 Å.

1. Introduction: Multi-walled carbon nanotubes (MWCNTs) and single-walled carbon nanotubes (SWCNTs) were first reported in 1991 and 1993, respectively [1, 2]. Carbon nanotubes (CNTs) are cylindrical macromolecules entirely comprising of carbon atoms, with a geometric configuration defined by a pair of integers (n , m), which are known as the chiral vector numbers [3]. The discovery of the CNTs has generated much interest owing to their outstanding physical and chemical properties such as a high electrical conductance, mechanical stiffness and light weight, leading to many possible applications such as field emission, electrochemical actuation and transistors [3, 4]. This has led to both single-walled and multiple-walled CNTs becoming the focus of intensive research interest as the possible electrodes to transmit electrical signals and as sensors to detect the concentrations of chemical or biological material [3–5]. The possibility of using the CNTs as engineered nanoscale flow channels has also attracted much attention in nanobiotechnology for the transport of water, proteins and macromolecules [6].

Watson and Crick [7] formulated the geometric model for the structure of deoxyribonucleic acid (DNA) in 1953, nearly one century after the discovery of DNA by Friedrich in 1869 [8], and it is now well established that the DNA molecule comprises of two long polynucleotide helical chains composed of four nucleotide subunits [7, 9]. In the case of the DNA, each nucleotide is composed of sugar attached to a single phosphate group with four possible bases; guanine (G), cytosine (C), adenine (A) and thymine (T) [9], respectively. DNA's unique features make it an important and a promising molecule with all the basic properties necessary for the self-assembly of the nanomaterial electronic devices [10]. By using the molecular recognition between the complementary strands of the double-strand DNA, various geometric objects at the nanometre scale have been constructed [11].

The functionalisation and the applications of CNTs and DNA have emerged as novel areas in biomechanics and biochemistry with promising thermodynamics, electronics, optics and magnetism [12]. In particular, the DNA molecule can be used to increase the CNT solubility in organic media and further applications and in the advancement of DNA-based nanostructures. The DNA molecule can also be used to distinguish the conducting from semi-conducting CNTs [13]. In addition, the DNA/CNT hybrids hold promise for new applications in many medical areas. For

example, the DNA/SWCNT can be used as vehicles for drug and gene delivery [14–16]. For these reasons, the interaction of the single-strand DNA (ssDNA) with the CNTs has been the subject of several studies. Gao *et al.* [17] investigated the dynamics of the ssDNA molecules being encapsulated inside the CNT by using the molecular dynamics (MD) simulations, and they found that the ssDNA molecule may be encapsulated inside a (10, 10) CNT. Pei *et al.* [18] employed the MD simulations to investigate the translocation of the ssDNA inside the CNT in water, and found that the ssDNA is unable to enter an (8, 8) CNT, but passes through larger CNTs with armchair chiralities in the range (10, 10)–(14, 14). Xue and Chen [6] also employed the MD simulations to study the translocation of the ssDNA molecules through the single-walled CNTs both ‘in vacuo’ and in an aqueous environment. They show that the insertion of the ssDNA molecule into a (10, 10) CNT is spontaneous within 100 ps in vacuo, but there is no corresponding spontaneous insertion of the ssDNA into the (10, 10) CNT for simulation times up to 2 ns at a temperature of 400 K and pressures of 3 bar in an aqueous environment. Kamiya and Okada [16] employed the density functional theory to investigate the encapsulation of the ssDNA inside the SWNTs, and found that the encapsulation reaction is exothermic for the nanotubes of radii larger than 6.15 Å. D'yachkov *et al.* [19] used a molecular docking method to study the complex formation of the ssDNA with the nanotubes as a function of the nucleotide composition of the DNA and the nanotube diameter, and found that a (14, 14) nanotube is too small for the ssDNA to enter.

Here, we adopt the 6–12 Lennard-Jones potential and the continuum approach which assumes that a discrete atomic structure can be replaced by an average atomic surface density of the atoms on the ssDNA molecule and an average surface density of the carbon atoms on the nanotube. We comment that Girifalco *et al.* [20] stated that the continuum Lennard-Jones approach may in many instances be a better approximation than a set of discrete atomic centres, since the former may be viewed as arising from an average over all the possible electronic configurations. We first examine the suction behaviour for the ssDNA entering a SWCNT, assumed to be semi-infinite in length, and because of the short range nature of the Lennard-Jones interactions, this is a reasonable approximation. Also, we determine the minimum potential energy equilibrium position for the ssDNA inside the SWCNT.

2. Energy between the ssDNA molecule and the CNT: We assume that an ssDNA has a helical geometry, and this assumption follows the previous experimental studies [21–24], as shown in Fig. 1. The unit cell of the ssDNA molecule used here is assumed to comprise of 10 nucleotides, which give a total of 377.75 atoms in the unit cell. These ten nucleotides comprise of 97.5 carbon, 142.5 hydrogen, 37.5 nitrogen, 90 oxygen and ten phosphorus atoms, which gives an average of 37.75 atoms per nucleotide. With reference to the rectangular Cartesian coordinate system (x, y, z), the ssDNA has the coordinates

$$H(\theta_1, t) = (rt \cos \theta_1, rt \sin \theta_1, c\theta_1/2\pi)$$

where the numerical value of r is the radius of the ssDNA helix and c is the unit cell length taken to be 5.4 and 34 Å, respectively [9, 17]. The parametric variable t is such that $0 < t < 1$ and $-\pi < \theta_1 < \pi$, respectively. We comment that a helical curve is normally parameterised by the single parameter θ_1 . In this case, we have adopted two parameters to allow for the variable internal points of the helicoid, so that we may integrate over all the values of the DNA radius from zero to r . We also comment that the ssDNA is a disordered polymer that is unlikely to have a precise helical conformation. In this Letter, we assume the ideal conformation as a first step towards modelling more realistic situations.

Similarly, with reference to the same rectangular Cartesian coordinate system (x, y, z) with the origin located at the centre of the nanotube, a typical point on the surface of the tube has the coordinates $(a \cos \theta_2, a \sin \theta_2, z)$, where a is the radius of the CNT and $0 < z < \infty$ and $-\pi < \theta_2 < \pi$, respectively. Here, we adopt the Lennard-Jones potential to determine the van der Waals interaction and the equilibrium position for the ssDNA inside the SWCNT. The classical Lennard-Jones potential interaction energy between a pair of atoms is given by

$$P(\rho) = -\frac{A}{\rho^6} + \frac{B}{\rho^{12}}$$

where A and B denote the attractive and the repulsive constants, respectively, and ρ denotes the distance from a typical point of the helicoid to a typical point on the cylindrical surface. The 6–12 Lennard-Jones potential may also be expressed as

$$P(\rho) = 4\epsilon \left[-\left(\frac{\sigma}{\rho}\right)^6 + \left(\frac{\sigma}{\rho}\right)^{12} \right]$$

where $\epsilon = A^2/4B$ is the magnitude of the energy at the equilibrium distance $\rho_0 = 2^{1/6}\sigma = (2B/A)^{1/6}$, and σ is the atomic distance when the potential energy is zero. By using the 6–12 Lennard-Jones potential, together with the continuum approximation, which assumes that the discrete atoms may be replaced by a uniform density of the atoms over the surface, the total non-bonded interaction energy E ,

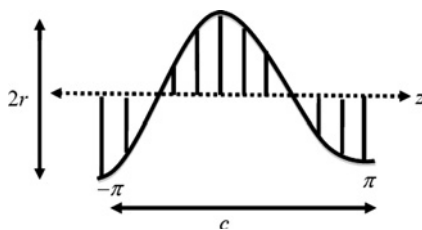


Figure 1 Assumed geometric profile of the ssDNA molecule

Table 1 Lennard-Jones constants [25]

	ϵ (eV $\times 10^{-2}$)	σ , Å	A , eV Å ⁶	B , eV Å ¹²
C–C	0.4119	3.88	56.21	191800
C–H	0.1336	3.54	10.52	20700
C–N	0.5089	3.788	60.09	177400
C–O	0.6197	3.695	63.08	160600
C–P	0.6197	4.088	115.6	539300

Table 2 Numerical values of the other constants

Constant	Value
radius of (8, 8)	5.4 Å
radius of (9, 9)	6.1 Å
radius of (10, 10)	6.8 Å
radius of (11, 11)	7.5 Å
radius of (12, 12)	8.1 Å
radius of (13, 13)	8.8 Å
radius of (14, 14)	9.5 Å
radius of (15, 15)	10.2 Å
radius of (16, 16)	10.9 Å
radius of ssDNA r	5.4 Å
length of ssDNA c	34 Å
mean surface density of the CNT	$\eta_g = 0.3812 \text{ Å}^{-2}$
mean surface density of the ssDNA	$\eta_d = 1.22 \text{ Å}^{-2}$
attractive constant CNT–DNA	$A = 42.56 \text{ eV Å}^6$
repulsive constant CNT–DNA	$B = 127500 \text{ eV Å}^{12}$

may be deduced from

$$E = \eta_1 \eta_2 \int_{S_1} \int_{S_2} \left(-\frac{A}{\rho^6} + \frac{B}{\rho^{12}} \right) dS_1 dS_2$$

where η_1 and η_2 denote the atomic surface densities of the first and the second molecules, respectively. The numerical values of the constants used throughout this Letter are given in Tables 1 and 2.

3. Suction energy ssDNA entering the CNT: In this Section, we determine the energy of the ssDNA molecule as it enters on axis into a SWCNT. The total work performed by the Lennard-Jones interaction on a molecule entering the CNT defines the suction energy. With reference to Fig. 2, the CNT is assumed to be semi-infinite in length and of radius a , with the parametric equations for the tube given by $(a \cos \theta_2, a \sin \theta_2, z)$. The ssDNA is assumed to be a helix of radius r and centred on the z -axis so that a typical point on the helicoid is located at the position $z = Z$ and offset from the z -axis by a distance ξ . Owing to the symmetry of the CNT we may without loss of generality denote this point by the coordinates $(\xi, 0, Z)$, where $\xi = rt$ and $Z = Z_0 + c\theta_1/2\pi$, respectively. Thus, the distance from a typical point of the ssDNA molecule to a typical point on the cylindrical surface is

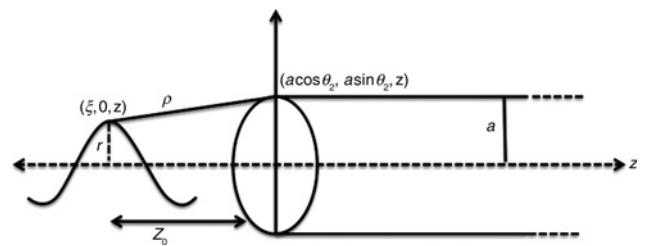


Figure 2 ssDNA molecule at the entrance to the SWCNT

given by

$$\begin{aligned}\rho^2 &= a^2 + \xi^2 - 2a\xi \cos \theta_2 + (z - Z)^2 \\ &= (a - \xi)^2 + 4a\xi \sin^2(\theta_2/2) + (z - Z)^2\end{aligned}$$

By using the Lennard-Jones interaction energy and the continuum approximation, the total interaction energy may be written as

$$\begin{aligned}E &= \frac{rcan_g\eta_d}{2\pi} \int_{-\pi}^{\pi} \int_{-\pi}^{\pi} \int_0^1 \int_0^{\infty} \left(-\frac{A}{\rho^6} + \frac{B}{\rho^{12}} \right) \\ &\quad \times \left[1 + \left(\frac{2\pi r}{c} \right)^2 t^2 \right]^{1/2} dz dt d\theta_1 d\theta_2\end{aligned}$$

where η_g and η_d represent the mean atomic surface densities of the CNT and the DNA, respectively. Furthermore, we define the integral T_n by

$$T_n = \int_{-\pi}^{\pi} \int_{-\pi}^{\pi} \int_0^1 \int_0^{\infty} \rho^{-n} \times \left[1 + \left(\frac{2\pi r}{c} \right)^2 t^2 \right]^{1/2} dz dt d\theta_1 d\theta_2 \quad (1)$$

to evaluate the integrals T_n analytically, we defined the integral J_n

$$J_n = \int_0^{\infty} [\alpha + (z - Z)^2]^{-n} dz$$

where $\alpha = (a - rt)^2 + 4art \sin^2(\theta_2/2)$ and $Z = Z_0 + c\theta_1/2\pi$, respectively, and by making the change of the variable $x = z - Z$ which gives

$$\begin{aligned}J_n &= \int_{-Z}^0 [\alpha + x^2]^{-n} dx + \int_0^{\infty} [\alpha + x^2]^{-n} dx \\ &= J_{n,1} + J_{n,2}\end{aligned}$$

For evaluating $J_{n,1}$ and $J_{n,2}$. We let $y = (x/Z)^2$ for $J_{n,1}$. We also make the substitution $X = x/a$, and then $v = X^2$ and $v = s/(1-s) \Rightarrow s = v/(1+v)$ for $J_{n,2}$, thus

$$J_{n,1} = -(1/2)Z\alpha^{-n} \int_0^1 y^{-1/2} [1 + (Z^2/\alpha)y]^{-n} dy$$

and

$$\begin{aligned}J_{n,2} &= (1/2)a\alpha^{-n} \int_0^1 s^{-1/2} (1-s)^{n-3/2} \\ &\quad \times [1 - (\alpha - a^2/\alpha)s]^{-n} ds\end{aligned}$$

using the definition of the hypergeometric function [26, §7.5], thus

$$J_{n,1} = -Z\alpha^{-n} F(n, 1/2; 3/2; -Z^2/\alpha)$$

and

$$J_{n,2} = \frac{a\sqrt{\pi}\alpha^{-n}\Gamma(n-1/2)}{2\Gamma(n)} F[n, 1/2; n; (\alpha - a^2/\alpha)]$$

where $F(a, b; c; z)$ is the standard hypergeometric function. By using the generalised hypergeometric series [27], we may deduce

$$J_{n,1} = -\sum_{i=0}^{\infty} \frac{(n)_i (1/2)_i}{i! (3/2)_i} (-1)^i Z^{2i+1} \alpha^{-n-i}$$

and

$$J_{n,2} = \frac{a\sqrt{\pi}\Gamma(n-1/2)}{2\Gamma(n)} \sum_{j=0}^{\infty} \frac{(1/2)_j}{j!} (\alpha - a^2)^j \alpha^{-n-j}$$

Now we can easily evaluate the integrals T_n over θ_1 , by defining the integral S_n

$$S_n = \int_{-\pi}^{\pi} (J_{n,1} + J_{n,2}) d\theta_1$$

thus

$$S_n^* = \pi/c(i+1) \left[(Z_0 + c/2)^{2i+2} - (Z_0 + c/2)^{2i+2} \right] + 2\pi$$

To evaluate the integrals T_n over θ_2 , we defined the integral W_n as

$$W_n = \int_{-\pi}^{\pi} (J_{n,1} + J_{n,2}) d\theta_2$$

and by introducing the integral $W_{n,1} = \int_{-\pi}^{\pi} J_{n,1} d\theta_2$, thus

$$W_{n,1}^* = \int_{-\pi}^{\pi} [\beta + \gamma \sin^2(\theta_2/2)]^{-n-i} d\theta_2 \quad (2)$$

where $\beta = (a - rt)^2$ and $\gamma = 4art$, respectively, and making the change of the variable $u = \theta_2/2$ gives

$$W_{n,1}^* = 4 \int_0^{\pi/2} [\beta + \gamma \sin^2(u)]^{-n-i} du$$

taking $\tau = \sin^2 u$, thus

$$\begin{aligned}W_{n,1}^* &= 2\pi\beta^{-n-i} F[n-i, 1/2; 1; -\gamma/\beta] \\ &= 2\pi \sum_{k=0}^{\infty} \frac{(n+i)_k (1/2)_k}{(k!)^2} (-1)^k \beta^{-n-i-k} \gamma^k\end{aligned}$$

Now, we introduce the integral $W_{n,2} = \int_{-\pi}^{\pi} J_{n,2} d\theta_2$, thus

$$W_{n,2}^* = \int_{-\pi}^{\pi} [\omega + \gamma \sin^2(\theta_2/2)]^j [\beta + \gamma \sin^2(\theta_2/2)]^j d\theta_2$$

where $\omega = -2art + r^2 t^2$, $\beta = (a - rt)^2$ and $\gamma = 4art$, respectively, and by making the change of the variables as shown in (2), $W_{n,2}^*$ becomes

$$\begin{aligned}W_{n,2}^* &= 2\omega^j \beta^{-n-j} \int_0^1 \chi^{-1/2} (1-\chi)^{-1/2} [1 + (\gamma/\omega)\chi]^j \\ &\quad \times [1 + (\gamma/\beta)\chi]^{-n-i} d\chi\end{aligned}$$

using the definition of an Appell hypergeometric function [28], thus

$$W_{n,2}^* = 2\pi\omega^j \beta^{-n-j} F_1[1/2; -j, n+j; 1; -\gamma/\omega; -\gamma/\beta]$$

by using the formula for the Appell hypergeometric function given in [28], which is given as

$$F_1(a'; b', b''; c'; x'; y') = \sum_{m'=0}^{\infty} \sum_{n'=0}^{\infty} \frac{(a')_{m'+n'} (b')_{m'} (b'')_{n'}}{m'! n'! (c')_{m'+n'}} x'^{m'} y'^{n'}$$

$W_{n,2}^*$ becomes

$$W_{n,2}^* = 2\pi \sum_{p=0}^{\infty} \sum_{q=0}^{\infty} \frac{(1/2)_{p+q} (-j)_p (n+j)_q}{(p!)^2 (q!)^2} \omega^{j-p} \beta^{-n-j-q}$$

To complete the evolution of the integrals T_n , we need to evaluate it over t . Hence, we defined the integral H_n as

$$H_n = \int_0^1 (J_{n,1} + J_{n,2}) (1 + \delta t^2)^{1/2} dt$$

where $\delta = (2r\pi/c)^2$, and by introducing the integral $H_{n,1} = \int_0^1 W_{n,1}^* (1 + \delta t^2)^{1/2} dt$

$$H_{n,1}^* = (4r)^k a^{-2(n+i)-k} \int_0^1 t^k [1 - (r/a)t]^{-2(n+i+k)} \times (1 + \delta t^2)^{1/2} dt$$

by expanding the term $[1 - (r/a)t]^{-2(n+i+k)}$

$$H_{n,1}^* = 4^k \sum_{g=0}^{\infty} \binom{-2(n+i+k)}{g} r^{k+g} a^{2(-n-i)-k-g} \times \int_0^1 t^{k+g} (1 + \delta t^2)^{1/2} dt$$

on making the substitution $\sigma = t^2$, $H_{n,1}^*$ becomes

$$H_{n,1}^* = 4^k / 2 \sum_{g=0}^{\infty} \binom{-2(n+i+k)}{g} r^{k+g} a^{2(-n-i)-k-g} \times \int_0^1 \sigma^{(k+g-1)/2} (1 + \delta \sigma)^{1/2} d\sigma$$

using the definition of the hypergeometric function [26, §7.5]

$$H_{n,1}^* = 4^k \sum_{g=0}^{\infty} \binom{-2(n+i+k)}{g} \frac{r^{k+g} a^{2(-n-i)-k-g}}{(k+g+1)} \times F\left(\frac{-1}{2}, \frac{k+g+1}{2}; \frac{k+g+3}{2}; -\delta\right)$$

Now, we introduce the integral $H_{n,2} = \int_0^1 W_{n,2}^* (1 + \delta t^2)^{1/2} dt$. We follow the same steps for evaluating $H_{n,1}^*$ above to evaluate $H_{n,2}^*$, and from which we find that the total interaction energy for the ssDNA molecule to be sucked into the CNT is given by

$$E = (rc\alpha\eta_g\eta_d/2\pi)(-AT_3 + BT_6) \quad (3)$$

3.1. Results and discussion: By using the algebraic software package MAPLE with the constants given in Table 2, the numerical calculations were performed, and in this Section, we present the numerical results showing the relationship between the interaction energy for the different sizes of the CNTs and an ssDNA molecule. Fig. 3 shows the relation between the distance

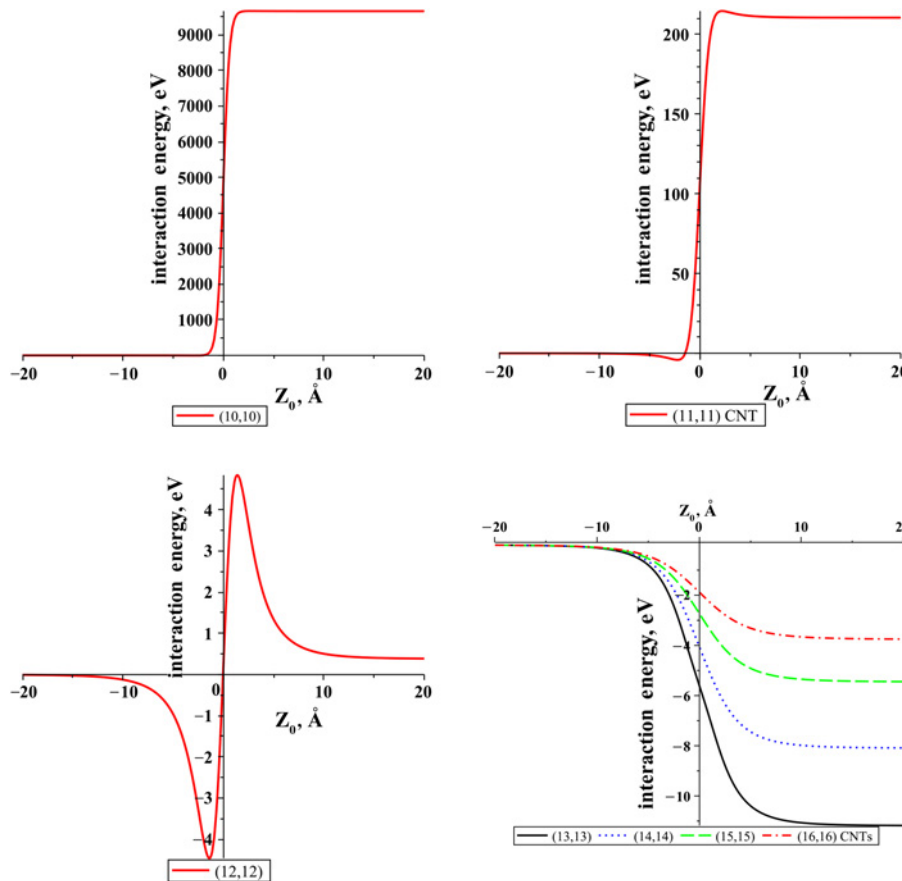


Figure 3 Interaction potential between the ssDNA molecule and the (10, 10)-(16, 16) CNTs

Z_0 and the interaction energy for the ssDNA molecule encapsulated into the armchair nanotubes in the range (10, 10)-(16, 16). From the open-end of the tube as given in Fig. 2 we observe that the lowest interaction energy occurs for the case of the (13, 13) nanotube. Also, for the (13, 13), the (14, 14), the (15, 15) and the (16, 16) CNTs we observe that the energetically most favourable location for the ssDNA molecule is inside the tube in the positive z direction giving rise to the possibility of the encapsulation of the ssDNA molecule in all these cases. In addition, Fig. 3 shows that there is no possibility of the encapsulation of the ssDNA molecule inside the (10, 10), the (11, 11) and the (12, 12) CNTs. These observations are in contrast to the results from [6], where they show that the ssDNA molecule could be inserted inside a (10, 10) CNT.

4. Preferred SWCNT to enclose the ssDNA: Here, we assume that the ssDNA molecule is symmetrically located on axis inside the CNT, and we look for the minimum interaction energy for the ssDNA molecule inside the SWCNT. We begin by considering the interaction of a single atom with the CNT assuming that the single atom is located at a distance ξ from the tube axis, as shown in Fig. 4. We then integrate the potential energy for the single atom over the surface of the DNA molecule. For the second integration we make the substitution $\xi = rt$ and the distance between the two typical points ρ is given by

$$\rho^2 = a^2 + \xi^2 + z^2 - 2a\xi \cos \theta_2$$

We have the interaction energy of the point with the infinite CNT from [29], which is given by

$$E_c = \frac{3\pi^2\eta_g}{4a^4} \left[-AF\left(\frac{5}{2}, \frac{5}{2}; 1; \left(\frac{\xi}{a}\right)^2\right) + \frac{21B}{32a^6} F\left(\frac{11}{2}, \frac{11}{2}; 1; \left(\frac{\xi}{a}\right)^2\right) \right]$$

Thus, the total potential energy of the dsDNA with the CNT per unit length E , is given by

$$E = \frac{rc\eta_d}{2\pi} \int_{-\pi}^{\pi} \int_0^1 E_c \left(1 + \frac{4r^2\pi^2}{c^2} t^2 \right)^{1/2} dt d\theta_1 \quad (4)$$

from which we find that the total interaction energy for the ssDNA inside the CNT is given by

$$E = \frac{3\pi^2 rc\eta_g\eta_d}{4a^4} \left(-AR_3 + \frac{21B}{32a^6} R_6 \right) \quad (5)$$

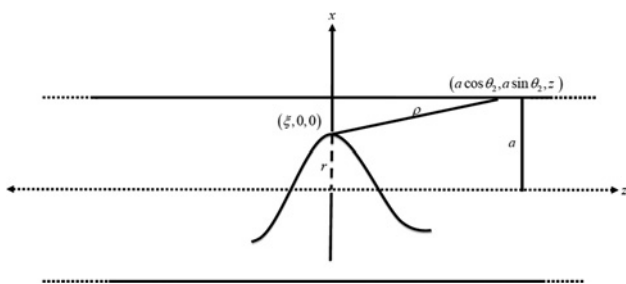


Figure 4 ssDNA molecule inside the SWCNT

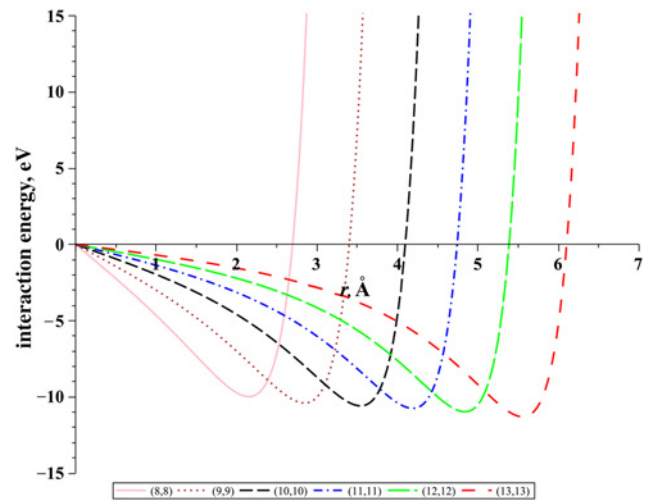


Figure 5 Interaction potential between the ssDNA molecule inside the (8, 8)-(13, 13) CNTs against ssDNA radius r

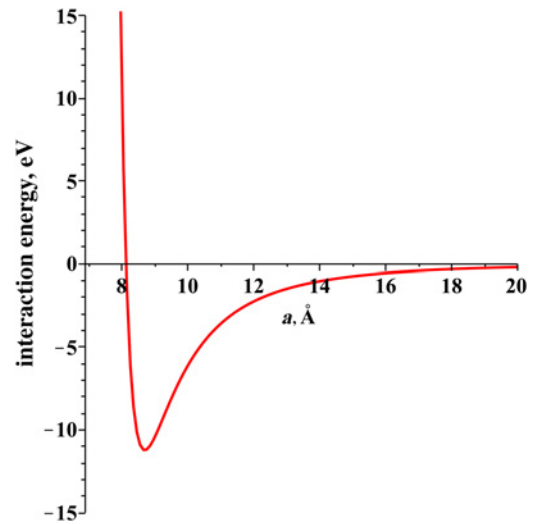


Figure 6 Interaction potential between the ssDNA molecule and the CNT against tube radius a

where R_n is given by

$$R_n = \sum_{k^*=0}^{\infty} \left[\frac{((2n-1)/2)_{k^*} r^{k^*}}{(2k^*+1)^{1/2} k^*! a^{k^*}} \right] \times F\left(-\frac{1}{2}, k^* + \frac{1}{2}; k^* + \frac{3}{2}; -\delta\right)$$

4.1. Results and discussion: By using the algebraic computer package MAPLE together with the constants given in Table 2, the numerical solutions for the ssDNA molecule inside the (8, 8)-(13, 13) CNTs are shown in Fig. 5 with respect to the radius of the ssDNA r . We observed that the minimum energy occurs at $r = 2.2$ Å, $r = 2.9$ Å, $r = 3.5$ Å, $r = 4.2$ Å, $r = 4.8$ Å and $r = 5.6$ Å, for the (8, 8)-(13, 13) CNTs, respectively. Also, we observe that at the point where the minimum energy occurs, the difference between the radii of the CNT and the DNA is ~ 3.3 Å ($a - r \simeq 3.3$ Å). In addition, Fig. 5 shows that the optimal radii of the ssDNA molecule to enclose inside the (8, 8)-(13, 13) CNTs are $r = 2.1$ Å, $r = 2.8$ Å, $r = 3.5$ Å, $r = 4.2$ Å, $r = 4.8$ Å and

$r = 5.6 \text{ \AA}$, respectively. In other words, Fig. 6 shows that the optimal radius of the CNT which is required to enclose the ssDNA with a radius of $\sim 5.4 \text{ \AA}$ is the (13, 13) CNT with a radius of $\sim 8.8 \text{ \AA}$, where the minimum energy occurs.

5. Summary: In this Letter, we present a model for the encapsulation of an ssDNA molecule inside a SWCNT by assuming a vacuum environment. We employ the 6–12 Lennard-Jones potential together with the continuum approximation to calculate the Lennard-Jones interaction energy, which we find may be expressed in terms of a series of hypergeometric functions. These analytical expressions can be readily evaluated numerically using the algebraic computer package MAPLE.

An expression for the suction energy of an ssDNA molecule assumed to enter on axis into a semi-infinite CNT is obtained. We observe that the suction behaviour depends on the radius of the CNT, and here we predict that it is less likely for an ssDNA molecule to be accepted into the CNT when the value of the tube radius is less than 8.1 \AA . In addition, we observe that the lowest interaction energy for all the CNTs considered in this Letter occurs for the (13, 13) CNT, assuming that the ssDNA molecule remains on the tube axis thus predicting the encapsulation of an ssDNA molecule into the (13, 13) CNT. This differs from [6, 17] which show that the ssDNA can be accepted inside a (10, 10) CNT. It also differs from [19] which shows that a (14, 14) nanotube diameter turns out to be too small for the ssDNA to enter into its cylindrical channel. The discrepancy between our results and these results may be attributed to the rigid geometric structure of the ssDNA which we have adopted here. Generally, there will be an elastic energy effect in the CNT as the ssDNA molecule enters the tube.

We also examined the interaction energy for an ssDNA inside the SWCNT for different armchair tubes, assuming that the ssDNA is already accepted into the CNT. The results indicate that the encapsulation of the ssDNA molecule into the SWCNTs may occur for the CNTs with a radii greater than 8.2 \AA . Moreover, the optimal radius of a CNT to enclose the ssDNA is $\sim 8.8 \text{ \AA}$, and we conclude that the preferred armchair tube is (13, 13). The benefit of the approach adopted here is the prediction of whether or not a certain DNA molecule will be encapsulated into a CNT, which will become an important issue for applications including drug and gene delivery research.

6. Acknowledgment: M. Alshehri gratefully acknowledges the King Saud University, Saudi Arabia for the awarding of a PhD scholarship.

7 References

- [1] Iijima S.: 'Helical microtubules of graphitic carbon', *Nature*, 1991, **354**, pp. 56–58
- [2] Iijima S., Ichihashi T.: 'Single-shell carbon nanotubes of 1-nm diameter', *Nature*, 1993, **363**, pp. 603–605
- [3] Dresselhaus M.S., Dresselhaus G., Avouris P.: 'Carbon nanotubes: synthesis, structure, properties and applications' (Springer, 2001), vol. 80
- [4] Hongjie D.: 'Carbon nanotubes: synthesis, integration, and properties', *Acc. Chem. Res.*, 2002, **35**, pp. 1035–1044
- [5] Huang W., Taylor S., Fu K., *ET AL.*: 'Attaching proteins to carbon nanotubes via diimide-activated amidation', *Nano Lett.*, 2002, **2**, pp. 311–314
- [6] Xue Y., Chen M.: 'Dynamics of molecules translocating through carbon nanotubes as nanofluidic channels', *Nanotechnology*, 2006, **17**, pp. 5216–5223
- [7] Watson J.D., Crick F.H.: 'Molecular structure of nucleic acids; a structure for deoxyribose nucleic acid', *Nature*, 1953, **171**, pp. 737–738
- [8] Dahm R.: 'Discovering DNA: Friedrich Miescher and the early years of nucleic acid research', *Hum. Genet.*, 2008, **122**, pp. 565–581
- [9] Alberts B., Johnson A., Lewis J., Raff M., Roberts K., Walter P.: 'Molecular biology of the cell' (Garland Science, New York, 2002, 4th edn)
- [10] Zheng M., Jagota A., Semke E.D., *ET AL.*: 'DNA-assisted dispersion and separation of carbon nanotubes', *Nature Mater.*, 2003, **2**, pp. 338–342
- [11] Seeman N.C.: 'DNA engineering and its application to nanotechnology', *Trends Biotechnol.*, 1999, **17**, pp. 437–443
- [12] Cui D.: 'Medicinal chemistry and pharmacological potential of fullerenes and carbon nanotubes, biomolecules functionalized carbon nanotubes and their applications'. Carbon Materials: Chemistry and Physics (Springer, The Netherlands, 2008), pp. 181–221
- [13] Li J., Ng H., Cassell A., *ET AL.*: 'Carbon nanotube nanoelectrode array for ultrasensitive DNA detection', *Nano Lett.*, 2003, **3**, pp. 597–602
- [14] Albertorio F., Hughes M., Golovchenko J., Branton D.: 'Base dependent DNA-carbon nanotube interactions: activation enthalpies and assembly-disassembly control', *Nanotechnology*, 2009, **20**, pp. 9
- [15] Benenson Y., Paz-Elizur T., Adar R., Keinan E., Livneh Z., Shapiro E.: 'Programmable and autonomous computing machine made of biomolecules', *Nature*, 2001, **414**, pp. 430–434
- [16] Kamiya K., Okada S.: 'Energetics and electronic structure of encapsulated single-stranded DNA in carbon nanotubes', *Phys. Rev. B*, 2011, **83**, p. 6
- [17] Gao H., Kong Y., Cui D., Ozkan C.S.: 'Spontaneous insertion of DNA oligonucleotides into carbon nanotubes', *Nano Lett.*, 2003, **3**, pp. 471–473
- [18] Pei Q.X., Lim C.G., Cheng Y., Gao H.: 'Molecular dynamics study on DNA oligonucleotide translocation through carbon nanotubes', *J. Chem. Phys.*, 2008, **129**, p. 125101
- [19] D'yachkov E., Dolin S., D'yachkov P.: 'Interaction of single-stranded DNA with carbon nanotubes according to the molecular docking method', *Dokl. Phys. Chem.*, 2008, **423**, pp. 297–301
- [20] Girifalco L.A., Hodak M., Lee R.S.: 'Carbon nanotubes, buckyballs, ropes, and a universal graphitic potential', *Phys. Rev. B*, 2000, **62**, pp. 104–110
- [21] Chen R.L.W., Fong P.: 'Helical configuration of single-stranded DNA', *J. Theor. Biol.*, 1969, **413**, pp. 180–187
- [22] Hingerty B., Broyde S.: 'Helix geometry of single stranded DNA "A" and "B" forms from minimum energy conformations of dimeric sub-units', *Nucleic Acids Res.*, 1978, **5**, pp. 127–137
- [23] Luzzati V., Mathis A., Masson F., Witz J.: 'Structure transitions observed in DNA and poly A in solution as a function of temperature and pH', *J. Mol. Biol.*, 1964, **10**, pp. 28–41
- [24] Duderstadt K.E., Chuang K., Berger J.M.: 'DNA stretching by bacterial initiators promotes replication origin opening', *Nature*, 2011, **478**, pp. 209–213
- [25] Mayo S.L., Olafson B.D., Goddard W.A.: 'DREIDING: a generic force field for molecular simulations', *J. Phys. Chem.*, 1990, **94**, pp. 8897–8909
- [26] Gradshteyn I.S., Ryzhik I.M.: 'Table of integrals, series, and products' (Academic Press, New York, 2007, 7th edn)
- [27] Erdelyi A., Magnus W., Oberhettinger F., Tricomi F.G.: 'Higher transcendental functions' (McGraw-Hill, USA, 1953), Vol. 1
- [28] Bailey W.N.: 'Generalized hypergeometric series' (Hafner Publishing Company, New York, 1964)
- [29] Cox B.J., Thamwattana N., Hill J.M.: 'Orientation of spheroidal fullerenes inside carbon nanotubes with potential applications as memory devices in nano-computing', *J. Phys. A, Math. Theory*, 2008, **41**, p. 27